Performance of a Solar Water Pump In Southern Part of Iran

M. Aghamohammadi, J. Zarinchang and M. Yaghoubi
Shiraz University, Shiraz, IRAN
Email: yaghoub@succ.shirazu.ac.ir

Abstract
In this study, performance of a solar water pump is analyzed. The pump under consideration has been installed in Khafr, in southern part of Iran. The system includes two cycles, the collector cycle and a Rankine cycle. R114 is used as a secondary fluid in a binary cycle engine. Flat plate collectors are employed to pump water by hydraulic transmission. For such configuration transient simulation is made for all components of the two cycles, and a specified model evaluates solar radiation for the location, and ambient condition are included from the local measurements. For each time step, inputs are, ambient temperature, solar radiation, geographical location and output are water and R114 temperature and mass flow rate at various locations in the cycle, collector plate temperature, efficiency of Rankine cycle and the overall efficiency of the solar pump. Finally theoretical results are compared with experimental measurements.

Key words: renewable energy, solar pump, thermal efficiency, Rankine cycle, collector.

Introduction

The French company (SOFRETES) has been one of the important solar water pump producers in 1970. In the first attempt SOFRETES has installed 25 Kw solar water pump for agricultural and drinking water purposes with 2.5 m^3/day in San Luis Delapaz of Mexico in 1975. During 1976, the company produced and installed more than forthy 1 Kw solar water pump in Eygept, India, Brazil, Senegal, Mali, Mauritania, and Nigeria. Each pump consisted a 100 m^2 flat collector, a two cylinders expansion engine, a hydraulic press and a diaphragm pump, which could pump 30 m^3 of water per day to a height of 20m [1].
During 1977, SOFRETES Company installed three units of solar water pumps in northern part, Yazd and Gelberenji in Iran. Gelberengi is a village, which is located in Khafr, 115-Km southern-east of Shiraz in Fars province. The pump was active for short period of time to supply drinking water. Later on, after Islamic revolution, the pump was replaced by an electric pump.

How the system works

Figure.1 shows different parts of the solar water pump. The system works as a binary Rankine vapor cycle. During a working cycle, a manual hand pump, pump water to collectors. The warm water passes from collector to main heat exchanger and then to a preheater. A feed pump from a storage tank in reverse direction of warm water will pump the liquid of R114. R114 will be changed to a superheat vapor in order to run the two-cylinder expansion engine. Water with lower temperature returns to collector while the R114 vapor with low pressure and temperature passes to a condenser. The fresh pumping water from the well will assist the condenser to change R144 vapor to liquid, and then water stored in a storage tank, which is located in 10 m above the ground level. Power output of the engine will run the liquid of R114 to heat exchanger, the collector circulation water pump and a hydraulic press which assists the diaphragm pump to pump water by a reciprocating column of water [2].

Computer Cycle Simulation

The governing equations for cycle simulation are as follow;
According to Daneshyar[3] for radiation in Iran we can write;

$$I_b = 950\{1 - \exp[-.075(90 - \theta_z)]\}, \quad \text{W/m}^2 \tag{1}$$

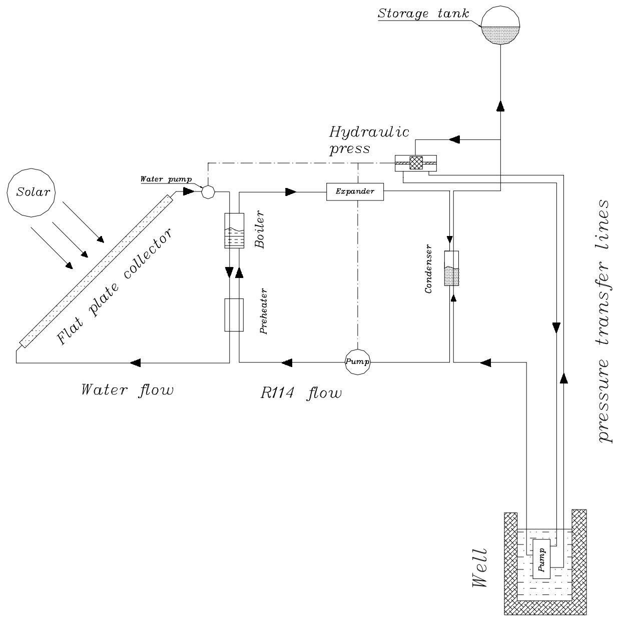

Fig.1- Solar water pump

$$I_d = 1.432 + 2.107(90 - \theta_z) + 121.3CF \tag{2}$$

$$I = (1 - CF)I_b \cos\theta_z + I_d \tag{3}$$

For flat plate collector based on Liu & Gordan[4] we can write,

$$I_T = I_b R_b \cos\theta_z + I_d \left(\frac{1 + \cos\beta}{2} \right) + I\rho_g \left(\frac{1 - \cos\beta}{2} \right) \tag{4}$$

Where $\beta = 25^o$

The cloud factor for different months of a year is shows in table 1.

Table 1. Values of cloud factor for various months in Shiraz

	Jan	Feb	Mar	Apr	Ma	Jun	Jul	Aug	Sep	Oct	Nov	Dec
Hajsaghati[5]	.342	.307	.347	.381	.313	.147	.195	.184	.131	.136	.239	.306
Karshenas[6]	.403	.391	.407	.457	.303	.151	.213	.2	.161	.209	.342	.4

The ambient temperature during each day is calculated by;

$$T_{amb} = \frac{(T_{max} + T_{min})}{2} + \frac{(T_{max} - T_{min})}{2} \times \sin\left[\frac{\pi}{12}(t - 9) \right] \tag{5}$$

The average monthly T_{max} , T_{min} for the location under consideration is shown in the table 2.

Table 2. The Values of monthly average maximum and minimum temperatures in Shiraz

	Jan	Feb	Mar	Apr	Ma	Jun	Jul	Aug	Sep	Oct	Nov	Dec
Maximum	20.6	18.5	18.9	27.7	34	39.7	42.8	41.8	39.7	35.3	28.7	25.7
Minimum	4.3	4.4	6.3	10.7	14	19.2	23.7	23.9	19.4	13.6	6.4	3.5

Thermal Analysis of Collector

Energy balance for absorber plate, before starting the cycle will be;

$$\left(\overline{mc}\right)_p \frac{d\overline{T}_p}{dt} = A_c\left[S - U_p\left(\overline{T}_p - \overline{T}_g\right)\right] \tag{6}$$

Energy balance for the glass of the collector is;

$$\left(\overline{mc}\right)_g \frac{d\overline{T}_g}{dt} = A_g\left[U_g\left(\overline{T}_g - \overline{T}_g\right) - U_\infty\left(\overline{T}_g - T_{amb}\right)\right] \tag{7}$$

If we assume that the heat loss from collector and glass are equal, then;

$$U_\infty A_c[\overline{T}_g - T_{amb}] = U_c A_c[\overline{T}_p - T_{amb}] \tag{8}$$

and for a certain ambient temperature from equation (8) we can write;

$$\frac{d\overline{T}_g}{dt} = \frac{U_c}{U_\infty}\frac{d\overline{T}_p}{dt} \tag{9}$$

From equations (6), (7), (9) we have a differential equation, which shows the temperature of absorber plate with time;

$$\overline{T}_p - T_{amb} = \frac{S}{U_c} - \left[\frac{S}{U_c} - \left(T_{p,o} - T_{amb}\right)\right]\exp\left[-\frac{U_c A_c t}{\left(\overline{mc}\right)_p + \left(\frac{U_c}{U_\infty}\right)_c\left(\overline{mc}\right)_g}\right] \tag{10}$$

After starting the cycle, the energy balance for collector's absorber plate is;

$$\left(mc\right)_p \frac{d\overline{T}_p}{dt} = A_c\left[S - U_l\left(\overline{T}_p - T_{amb}\right)\right] - Q_u \tag{11}$$

By solving the above equation with modified Euler method we can get the collector temperature as a function of time. The performance of main heat exchanger and preheater can be calculated by energy balance and application of ε - NTU method.

The governing equation for expansion engine and pumps are as follows;

The engine power output;

$$\dot{W}_{exp} = \eta_i \eta_m \dot{m}_o (h_{io} - h_{eo}) \tag{12}$$

The power for feed pump in the Rankine cycle is;

$$W_{feedpump} = \frac{\dot{m}_o\, \upsilon\left(P_{boiler} - P_{condenser}\right)}{\eta_{feedpump}} \tag{13}$$

Power for pump in the water well is;

$$W_{pump} = \frac{\dot{m}_w g\left(h_1 + h_2\right)}{\eta_{pump}} \tag{14}$$

The design conditions for the installed unit are;

Total radiation =850 W/m^2,

Total collector area =80 m^2,

Total working hours =4-6 hour/day,

Collector tilt angle =25°,

Head to pump the water =30m, and

Well output =3 m^3/hour.

With solution of above equations in a computer program and by entering the data such as, ambient temperature, wind velocity, solar radiation, geographical condition (28.5° geographical latitude), geometrical specification of different parts of the cycle, starting conditions: temperature 65 °C, pressure 7 bar in boiler, the output data of the collector for each minute interval of running cycle is determined. According to the initial starting condition, the unknown parameters such as mass flow rate and temperature of water and R114, engine power output, Rankine cycle efficiency, collector efficiency, useful energy are calculated for a period of working hours of the average day of each month.

Results

Figures 2 to 9 show results of simulation of the system for different month of a year. Calculation has been illustrated for the hottest and the coldest month of the year.

Figures 2&3 show the temperature variation of absorption plate, collector inlet and outlet water temperature, and boiler temperature during the hottest month (July) and coldest month (January) of the year. As the sun rises, temperature of the collector will rise until it reaches to the working temperature. After circulating water in the collector by a manual hand pump for 10 to 15 minutes, temperature of absorber plate sharply drops. Since, water absorbs heat from absorber plate, then the water temperature will drop but the temperature profile will be similar. Since the boiler temperature is related to the approach temperature between water and R114, therefore the boiler temperature will change similarly.

Figures 4&5 show the received radiation to collector and useful energy of the collector for July and January. Parameters, which affect the useful energy of collector, are: inlet temperature, received radiation of collector and water flow rate. These parameters will change simultaneously. Figure.4 shows that collector will work at a lower temperature; therefore the collector losses are low. But the effects of solar radiation and flow rate are a mather that overcome the collector losses, then the useful energy and efficiency will be maximum at noon. In summer time (i.e. July) the inlet temperature of collector is high about 75 ˚C to 90 ˚C. Collector will work at higher temperature, heat loss will increase and it overcomes the positive effects of solar radiation and water flow rate. Then the useful energy and collector efficiency would be minimum at noon.

Figures 6&7 show the variation of collector efficiency, Rankine cycle efficiency and overall efficiency for January and July. These figures show that collector efficiency will change between 25% to 35% during a year. Rankine cycle efficiency will be 8% to 10% during winter and 13% to 15% during summer time. This is due to boiler temperature at higher level than wintertime. Overall cycle efficiency will be 3% to 4% during the year. The low efficiency is a characteristic of solar system. Some times this efficiency will be less than 1% [7].

Figures 8&9 show the variation of collector's flow rate and water well output in the average day of January and July. Three pumps in the system, water feed pump of collector, R114 feed pump and diaphragm pump in the well operates by expansion Rankine engine. The power to these pumps depends on the variation of power output of the expansion engine during the day.

Figures.8&9 show that before starting the system, the flow rate of collector, R114 flow rate and output of the water well will increase from zero to a certain level, later on the variation will be the same as the variation in figures 6&7. Comparison of theoretical and experimental measurement of boiler pressure is made in figure 10, for the month of July. Maximum difference is 10%. It shows that simulation accurately predicts cycle pressure of the system.

Total performance of the system during a year is predicted in figure 11. It is observed that average output of well during a year is 20 m^3/day, average efficiency of system is 2.804% and average mass flow rate of water of well is 1.285 Kg/s.

Conclusion

Based on the thermal simulation made, following conclusion can be drawn.

1) Average water well output would be 35 m^3 in July and 12 m^3 in January.
2) In the solar system with electric pump, the collector flow rate is constant, while in the system under consideration; temperature and flow rate of the collector is not constant.
3) The average working hours and flow rate of the system in Khafr are 4-6 hours and 20 m^3 /day. The overall efficiency of the cycle is 2.804%, which corresponds to SOFRETES recommendation.

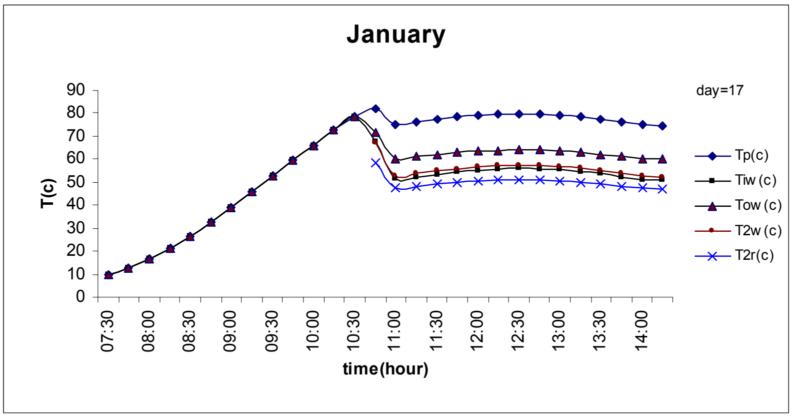

Fig.2- Temperature of: absorber plate, collector water inlet & outlet, water outlet of boiler and R114 in boiler

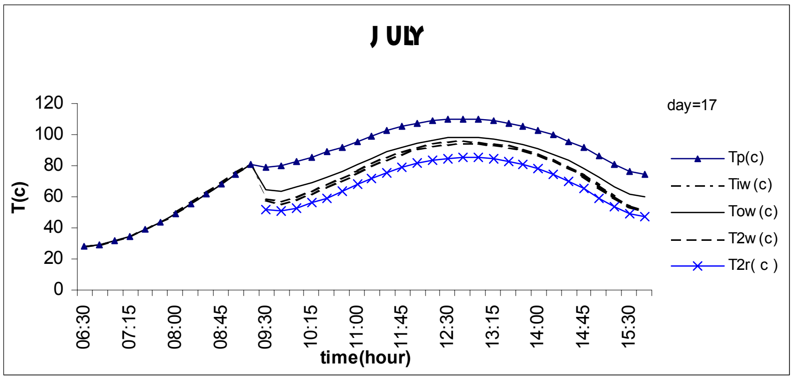

Fig.3- Temperature of: absorber plate, collector water inlet & outlet, water outlet of boiler and R114 in boiler

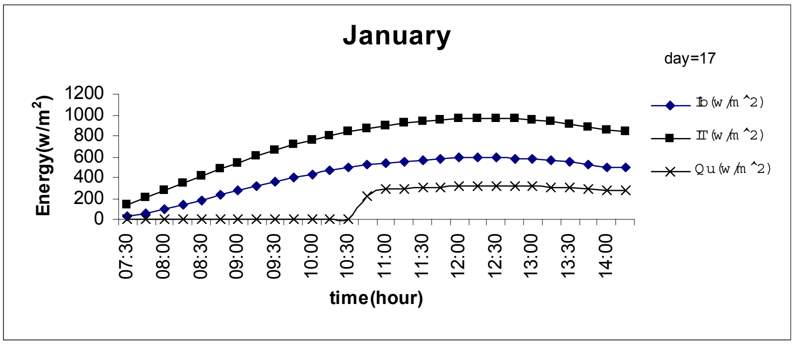

Fig.4- Beam, Total incident radiation and Collector useful energy In January

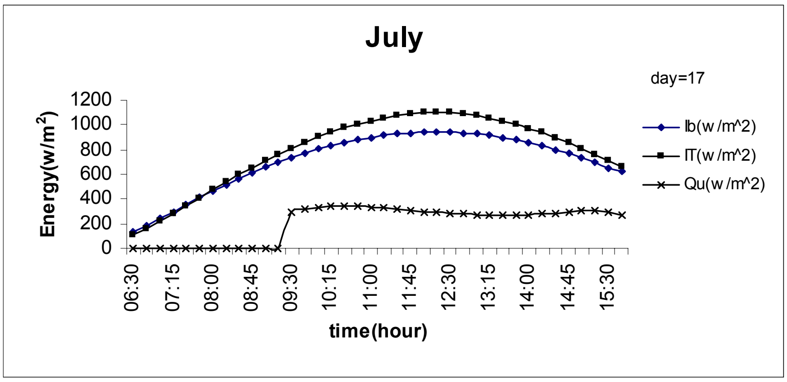

Fig.5- Beam, total incident radiation and collector useful energy In July

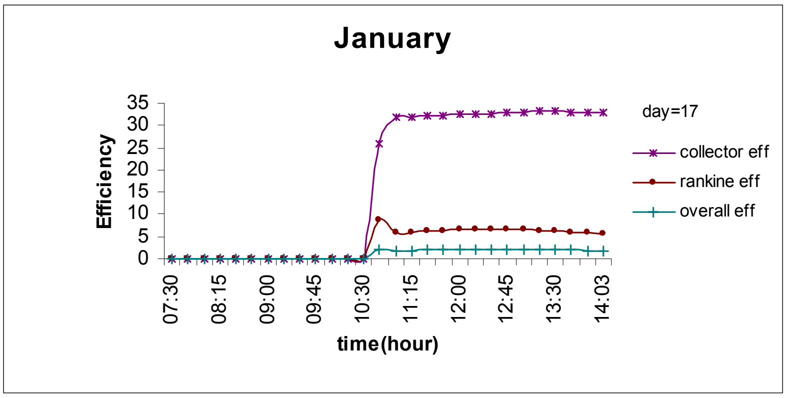

Fig.6- Collector efficiency, Rankine efficiency and overall efficiency of the system in January

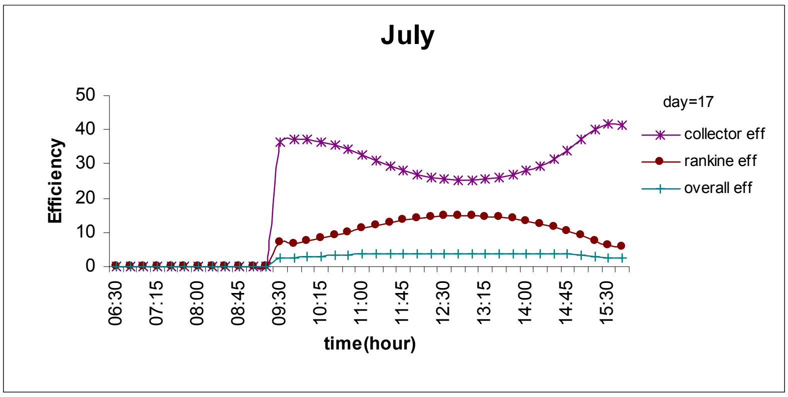

Fig.7– Collector efficiency, Rankine efficiency and overall efficiency of the system in July

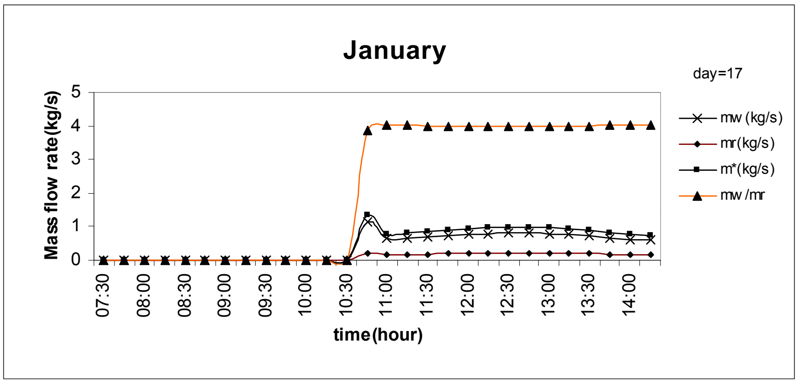

Fig.8- Mass flow rate of: collector, R114 and water well and the ratio

Of m_w / m_r in January.

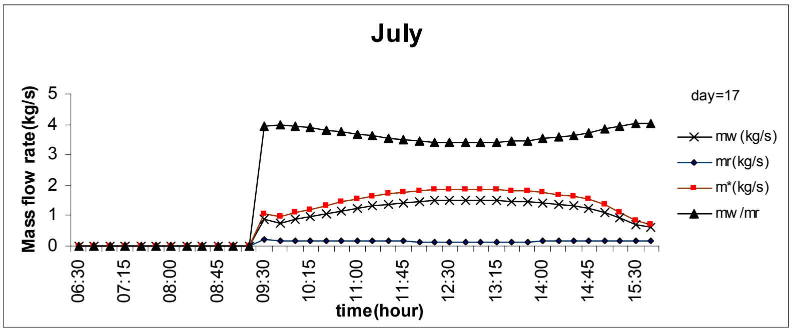

Fig.9- Mass flow rate of; collector, R114 and water well and the ratio

Of m_w / m_r in July.

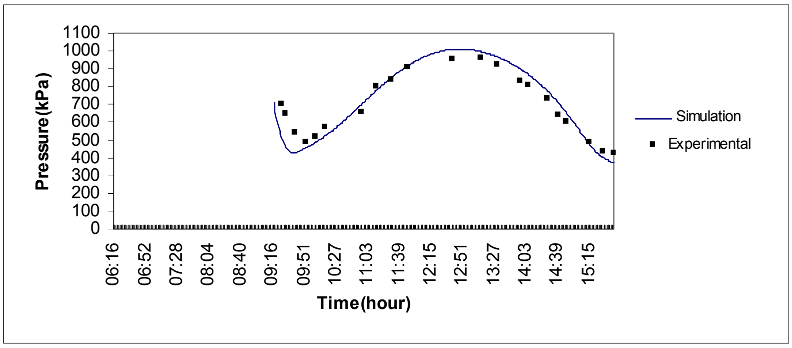

Fig.10- Comparison of theoretical prediction and experimental measurements of pressure in the boiler

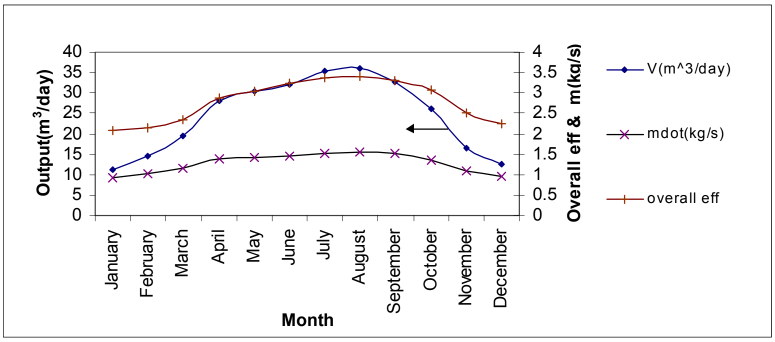

Fig.11- Yearly performance of solar pump for Khafr

Nomenclature

A_c Area of collector, (m^2).

CF Cloud Factor.

h_{io} The enthalpy of organic fluid at expander inlet,(J/°k).

h_{eo} The enthalpy of organic fluid at expander outlet, (J/°k).

h_1 Static head from the depth of well to storage tank, (m).

h_2 Friction losses in pipes, (m).

I Incident total radiation on the horizontal plate, (W/m^2)

I_b Beam radiation, (W/m^2).

I_d Diffuse radiation, (W/m^2).

I_T Incident total radiation on the inclined plate, (W/m^2).

$(\overline{mc})_g$ Heat capacity of glass, (J/°k).

$(\overline{mc})_p$ The heat capacity of plate,(J/°k).

$\dot{m}_o$ Organic fluid mass flow rate, (Kg/s).

$\dot{m}_w$ Water mass flow rate, (Kg/s).

Q_u Useful energy of collector, W.

S Absorbed radiation by plate, (W/m^2).

T_{amb} Ambient temperature, (˚k).

$\overline{T}_p$ Plate average temperature (˚k).

U_c Overall heat transfer coefficient from collector to ambient, (W/m^2.° k).

U_p Overall heat transfer coefficient from plate to cover, (W/m^2.k).

U_∞ Overall heat transfer coefficient from cover to, (W/m^2.k).

$\dot{W}_p$ Pump power,W.

$\dot{W}_{exp}$ Expander power,W.

$\eta_{feedpump}$ Feed pump efficiency, (65%).

η_i Isentropic efficiency, (95%).

η_m Mechanical efficiency, (90%).

η_{pump} Well pump efficiency, (65%).

θ_z Zenith angle.

ρ_g Ground reflectivity.

References

1- Grag, H. P., 1987. Advances in Solar Energy Technology. London. Printice – Hall.
2- Bahadori, M.N., 1987, Solar Water Pumping, Solar Energy, **21**: 307-316.
3- Daneshyar, M., 1978, Soalr Radiation for Iran, Solar Energy, **21**: 345-353.
4- Duffie, J.A., W.A., Beckman, 1991. Solar Engineering of Thermal Processe. New York. John Wiley & Sons.
5- Hajsaghati, A., 1991. Solar Energy Designs in Iran, Tehran.
6- Karshenas, M., 1998. Available Solar Energy in Iran, Shiraz.
1- Spindler, K., K. Chandwalker and E. Hahne, 1996, Small Solar (Thermal) Water Pumping System, Solar Energy, **57**: 69-76.